INT. J. REMOTE SENSING, 10 MAY, 2004,
VOL. 25, NO. 9, 1685–1700

Taylor & Francis
Taylor & Francis Group

Using artificial neural networks to map the spatial distribution of understorey bamboo from remote sensing data

M. LINDERMAN*†, J. LIU†, J. QI‡, L. AN†, Z. OUYANG§, J. YANG¶ and Y. TAN¶

†Department of Fisheries & Wildlife, Michigan State University, East Lansing, MI 48824, USA
‡Department of Geography, Michigan State University, USA
§Department of Systems Ecology, Research Center for Eco-Environmental Sciences, Chinese Academy of Sciences, Beijing, China
¶Wolong Giant Panda Research Center, Sichuan, China

(Received 3 January 2002; in final form 14 May 2003)

Abstract. Understorey vegetation is a critical component of biodiversity and an essential habitat component for many wildlife species. However, compared to overstorey, information about understorey vegetation distribution is scant, available mainly over small areas or through imprecise large area maps from tedious and time-consuming field surveys. A practical approach to classifying understorey vegetation from remote sensing data is needed for more accurate habitat analyses and biodiversity estimates. As a case study, we mapped the spatial distribution of understorey bamboo in Wolong Nature Reserve (south-western China) using remote sensing data from a leaf-on or growing season. Training on a limited set of ground data and using widely available Landsat TM data as input, a nonlinear artificial neural network achieved a classification accuracy of 80% despite the presence of co-occurring mid-storey and understorey vegetation. These results suggest that the influences of understorey vegetation on remote sensing data are available to practical approaches to classifying understorey vegetation. The success here to map bamboo distribution has important implications for giant panda conservation and provides a good foundation for developing methods to map the spatial distributions of other understorey plant species.

1. Introduction

Understorey vegetation is a significant component of biological diversity and critical habitat for countless wildlife species (MacArthur and MacArthur 1961, Odum 1971, Schaller *et al.* 1985). However, monitoring of understorey conditions has been restricted to tedious and time-consuming ground surveys due to a lack of alternative methods such as remote sensing. More specifically, whereas significant advances in regional ecology have been made from overstorey mapping (Roughgarden *et al.* 1991), extensive spatial distribution information of understorey vegetation has remained unavailable due to the limitations of traditional remote sensing classification techniques. In this study we examined the feasibility of using artificial

*Corresponding author; tel: 517 353 5468; fax: 517 432 1699; e-mail: linderm5@msu.edu

International Journal of Remote Sensing
ISSN 0143-1161 print/ISSN 1366-5901 online
http://www.tandf.co.uk/journals
DOI: 10.1080/01431160310001598971

neural networks to classify understorey vegetation from optical remote sensing data based on limited field samples.

Studies have shown that canopy background features have a significant influence on optical radiance measured by remote sensors even under considerable cover (Huete *et al*. 1985, Ranson *et al*. 1986, Guyot and Riom 1989, Bausch 1993). In the near-infrared region, understorey can dominate the overall reflectance from open-canopy stands (Nemani *et al*. 1993). Studies on the relationship of Leaf Area Index (LAI) values to optical data have shown that, even in canopies up to 89% closed, understorey vegetation characteristics have a measurable effect on the radiance response recorded by a satellite sensor (Nemani *et al*. 1993, Law and Waring 1994, Spanner *et al*. 1994, Qi *et al*. 2000). However, the influence from background features is a function not only of the direct reflectance from gaps in the canopy, but also multiscattering between understorey and the overstorey as well as transmission through the canopy and is therefore a complex combination of linear and nonlinear overstorey and understorey contributions (Borel and Gerstl 1994). Therefore, while understorey vegetation and background features influence the response measured at distant sensors, the understorey is often not amendable to traditional classification techniques.

Most standard statistical classification techniques are restricted by underlying assumptions of the data (Atkinson and Tatnall 1997) and are often limited in their applications and accuracy for classifying complex scenes (Lillesand and Kiefer 1994). This becomes particularly relevant when considering the complex contributions of understorey vegetation. Attempts to use traditional methods to map understorey vegetation, even a coniferous understorey with a leaf-off deciduous overstorey, have had, at best, mixed results (Stenback and Congalton 1990, Porwall and Roy 1991, Ghitter *et al*. 1995). The degrees of linear and nonlinear contributions vary relative to the understorey and overstorey cover, structure, and other variables. In addition, changes in canopy cover and species composition, and understorey species composition and cover from pixel to pixel result in a complex distribution of understorey classes within the feature space.

Spectral unmixing methods, such as linear mixture models and artificial neural networks, have been shown to be able to parse the proportional effects of individual canopy features from the radiance response of a single heterogeneous pixel (Cross *et al*. 1991, Adams *et al*. 1995, Carpenter *et al*. 1999). These approaches are likely to be more amenable to classifying understorey vegetation. However, linear mixture models are sensitive to the nonlinear contributions of understorey vegetation. Past studies using the linear model have had to ignore or assume that the nonlinear interactions are small (Roberts *et al*. 1993, Asner and Lobell 2000, Gilabert *et al*. 2000). Artificial neural networks, on the other hand, in some situations significantly increased the ability to deconvolve the proportional influence of overstorey features in part by allowing for nonlinear effects (Foody 1996, Carpenter *et al*. 1999).

Artificial neural networks may provide a practical approach to understorey classification. Neural networks are essentially non-parametric data transformations that are not restricted by underlying assumptions and can account for nonlinear effects given a sufficiently complex partitioning of the classification space (Atkinson and Tatnall 1997). Furthermore, neural networks are more likely to learn the complex variability in the signature due to varying canopy and understorey conditions and to do so more efficiently than traditional classifications (Foody and Arora 1997, Atkinson and Tatnall 1997). To test the practicality of classifying understorey vegetation based on limited ground data, we compared the ability of an

artificial neural network to predict the presence or absence of understorey vegetation from optical remote sensing data relative to traditional techniques.

2. Study Area

The impetus for this study was the need for a practical method to classify the spatial distribution of understorey bamboo irrespective of the canopy conditions over large regions. Bamboo plays a vital role in the survival of the endangered giant panda (*Ailuropoda melanoleuca*) (Schaller *et al*. 1985, Liu *et al*. 1999a). The impact of the spatial distribution of bamboo on panda populations has been well-documented (Johnson *et al*. 1988, Taylor and Qin 1997). However, past panda habitat analyses have been limited in their ability to conduct accurate habitat assessments over large areas due to the lack of bamboo distribution maps with sufficient detail or extent as shown in figure 1 (Liu *et al*. 2001).

Remote sensing would be a preferable method for data acquisition at larger scales. However, methods to map the extent of bamboo, even employing aerial photography, have not been successful (Morain 1986, De Wulf *et al*. 1988, Porwall and Roy 1991). The main problem in classifying bamboo in much of the panda range is that it is typically found as an understorey species under variable canopy species, percentage cover and densities. We required an approach that would be able to classify the presence/absence of understorey bamboo irrespective of the overstorey.

Located between 102°52′ and 103°24′ E and 30°45′ and 31°25′ N in the Qionglai Mountains of south-western China, the reserve is approximately 200 000 ha in size and one of the largest parks dedicated to giant panda preservation (Liu *et al*. 1999b, Liu *et al*. 2001). It is estimated that approximately 10% of the total wild panda population can be found within this reserve. Within Wolong, elevations range from 1200–6525 m, creating several climatic zones and consequently high habitat diversity. From the lowest elevation to approximately 1600 m, the canopy consists mainly of evergreen broadleaf. From 1600–2000 m there is an increasing mixture of the broadleaf and deciduous. The canopy is dominated by deciduous vegetation from 2000 m to about 3600 m with an increasing mix from conifer at the higher altitudes. Above this elevation, subalpine conifers give way to alpine meadow at an elevation of approximately 4400 m. Throughout the reserve forest canopies averaged 56% closure and rarely exceed 90%, maintaining significant gap areas for light penetration.

Within the reserve, bamboo occurs up to an elevation of 4500 m and is typically an understorey species. Up to 11 species of bamboo are found in Wolong with two species, *Bashania fangiana* and *Fargesia robusta*, predominating (Schaller *et al*. 1985) (figure 2). In forested areas, bamboo is distributed in patches ranging in size from single plants to hundreds of metres across. Where bamboo occurs, it averages 41% of the ground cover. However, the spatial distribution of bamboo seemingly does not follow any trends relative to overstorey or abiotic factors (Reid *et al*. 1989). Regression relationships based on ground samples of overstorey cover, slope, altitude and bamboo ground cover in forested areas are shown in table 1 and suggest that the prediction of bamboo presence/absence is independent of within-stand characteristics. The lack of correlation of the spatial distribution of bamboo and environmental factors may be partly due to the unique episodic synchronized die-offs of large areas of bamboo (Reid *et al*. 1989, Keeley and Bond 1999). However, it is precisely this distribution that affects pandas.

The spatial distribution of bamboo is also influenced by human activities and

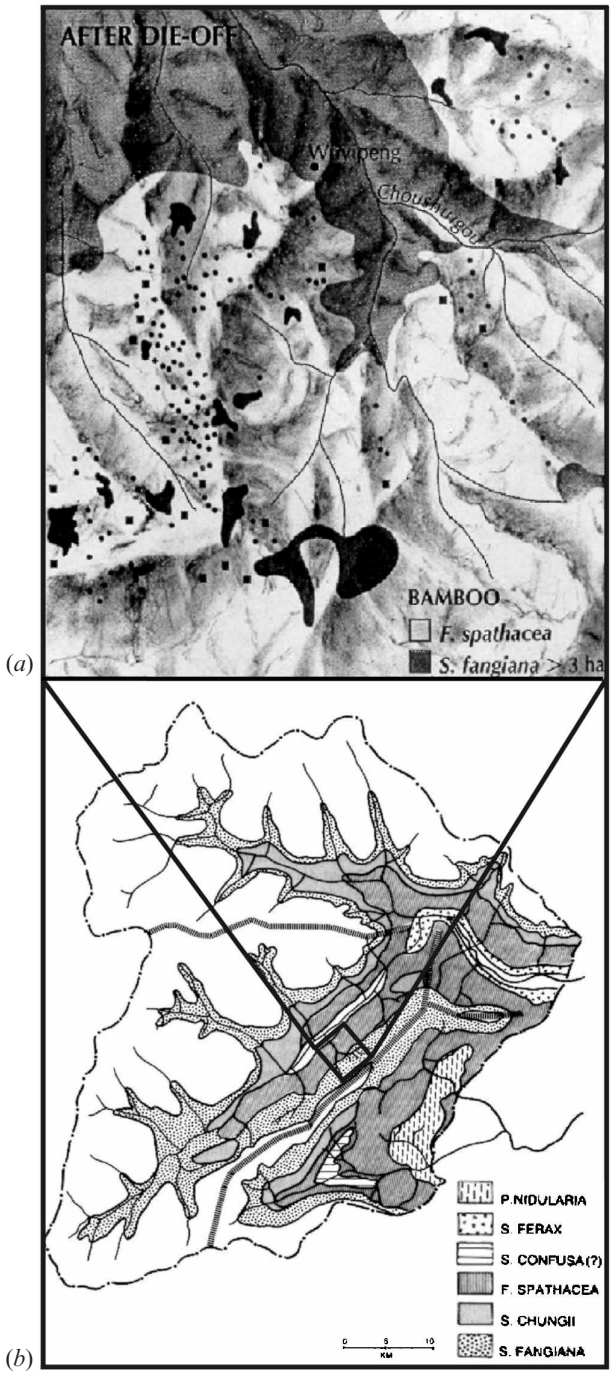

Figure 1. Examples of past bamboo distribution maps for Wolong Nature Reserve. Figure 1(*b*) shows the full-reserve map derived from field survey work conducted from 1979–1983 (Schaller *et al*. 1985 (reprinted with the permission of the University of Chicago Press)). The inset (figure 1(*a*)) shows the approximate area of the map shown in figure 1(*b*), a higher detail, smaller extent map derived from work done by Johnson *et al*. (1988) in response to a mass die-off of *Bashania fangiana* within the reserve.

(*a*) (*b*)

Figure 2. Examples of (*a*) *Bashania fangiana* beneath a typical overstorey and (*b*) *Fargesia robusta* with co-occurring vegetation.

restricted environmentally (e.g. high-altitude permanent rock, alpine meadow). Grazing and agricultural use have effectively removed bamboo from some areas. Other regions have been clear-cut leaving a mixed mid-storey shrub layer and a lower occurrence of bamboo. Finally, selective logging has changed the species composition of the overstorey and reduced canopy cover in some areas. While relatively limited in impact, these human activities are transforming the landscape and introducing additional complexity in classifying the land cover. The complex relationships between land cover and the lack of substantial correlation between the presence of bamboo and canopy conditions made prediction or classification using traditional methods difficult and required a new approach for accurate classification.

3. Methods

3.1. *Data*

Field data were collected throughout the reserve during the summers of 1998 and 1999. They included vegetation ground sampling plots for algorithm training

Table 1. Relationship between overstorey species and abiotic factors and understorey bamboo. Mean values show average values measured throughout the reserve. R and R^2 values show regression relationships between the given variable and the occurrence of bamboo.

	Bamboo (%)	Canopy (%)	Slope (°)	Altitude (m)
Mean	41.2 ± 36.2	55.6 ± 20.8	23.0 ± 10.7	2583 ± 285
R		0.11	0.30	0.14
R^2		0.01	0.09	0.02

and validation and ground control points (GCPs) to allow registration of the remote sensing data. Landsat Thematic Mapper (TM) data acquired over Wolong Nature Reserve in September 1997 were used for this study. The Landsat TM scene was registered to UTM WGS-84 coordinates to allow co-registration of the ground data. The remote sensing data were registered using the GCPs collected to an rms error (RMSE) of less than one pixel. To gather representative ground data, stratified sampling of the land covers and understorey conditions was conducted. Ground sample plots were located where access was possible and registered to the remote sensing data through differential Global Positioning System (GPS) using Trimble Pro XRS and Community Base Station receivers.

Plots were selected where the vegetation was relatively homogeneous over a $60\,m \times 60\,m$ area. A sample area was considered relatively homogeneous where similar percentages of vegetation were distributed evenly throughout the entire sample plot. Therefore, any $30\,m \times 30\,m$ subplot would contain the same vegetation percentages regardless of where it was situated within the $60\,m \times 60\,m$ plot. The $60\,m \times 60\,m$ dimensions were chosen to ensure that one pixel of the Landsat TM data (30 meter resolution) would be fully contained within a sample plot as prior knowledge of the GPS position in relation to the remote sensing grid was unknown. For each plot, information on the biota such as vegetation types for the overstorey, mid-storey and understorey, as well as the corresponding percentage cover, were recorded. Percentages of vegetation cover in the overstorey ($>5\,m$), mid-storey (2–5 m), and understorey ($<2\,m$) were estimated visually for the 60 m plots.

Training data for the artificial neural network were selected from the vegetation ground data where positions were known at a suitable accuracy (field data were filtered for GPS measurements with standard deviations greater than 10 metres) and stratified to include a representative sample of vegetation conditions. On this basis 189 sample plots were chosen. Approximately, two-thirds of these data were used to train the neural network and the remaining third reserved for validation. The data were categorized into presence/absence categories. If bamboo cover was greater than 10%, the training value was assigned a 1 (presence). Otherwise, the training value was assigned a 0 (absence). Such categorization was done for three reasons. First, sampling methods were limited in assigning absolute ground cover percentages over large sample plots. Second, at less than 10%, the cover was extremely insignificant, did not provide any useable biomass for pandas, and was considered to have a limited influence on the spectral response. And third, it was anticipated that a binary categorization would reduce data transformation complexity.

3.2. *Artificial neural network design*

For this study, the neural networks were simulated in the Neural Network module of Mathworks MATLAB (The MathWorks Inc. 1999). The back-propagation multilayer perceptron (MLP) is a commonly used and widely available neural network structure in remote sensing and was used in this study (Atkinson and Tatnall 1997) (figure 3).

Several variations of internal network structure, input data, and learning algorithms were tested to determine optimal algorithm characteristics. Different combinations of the Landsat TM (6 bands excluding thermal band) were examined as potential data input. As a result, the input layer consisted of three to six input nodes depending on the layers used. The structure of the hidden layers was also

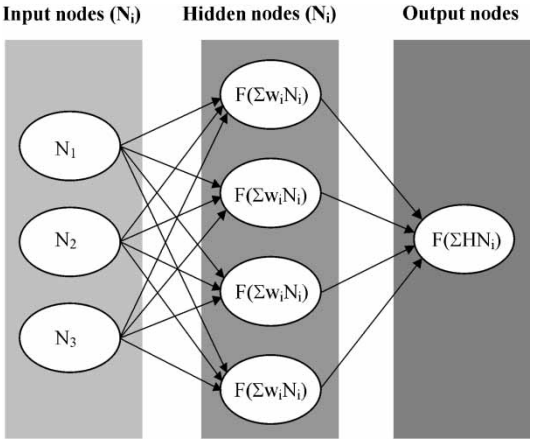

Figure 3. Representative schematic of an artificial neural network. The arrows represent a feed-forward process of transforming input data, such as remote sensing imagery, to an output space (e.g. bamboo existence/absence). Networks are trained through *a priori* knowledge of output and input relations (ground data and corresponding remote sensing pixel values) and a reiterative back-propagation of training errors to update the hidden layer weights.

tested to determine the necessary number of hidden layers and number of nodes per layer required. In addition, generalization techniques, methods to reduce over-fitting, were analysed including techniques such as early stopping by adjusting the training mean square error (MSE) goal and automated regularization utilizing the Bayesian Regularization (BR) learning algorithm. Early stopping, as the term suggests, establishes a higher error convergence threshold and thus stops the training process before full convergence occurs. This can be done automatically by comparing an additional reserved data set to determine when error minimization reduces generalization of the full data set. However, since training data were limited, preset early stopping error levels of 1×10^{-05} and 1×10^{-08} were tested relative to a full convergence level, typically around 1×10^{-20} (known from preliminary trials).

3.3. *Performance evaluation*

Evaluation of individual algorithms was conducted by examining algorithm performance through each of the four stages: training, simulation, verification and validation. The algorithms were first presented with training data (i.e. remote sensing pixel values and corresponding ground data of presence/absence values). If the algorithm was able to converge on the preset error goal, a $15\,\text{km} \times 15\,\text{km}$ evaluation subset of the remote sensing data was fed through the trained data, or simulated, to output a predicted map of bamboo presence/absence. This output subset was then examined to determine how well the predicted values conformed to the expected output values of 0 or 1. As in many practical applications, it was not possible to collect a completely representative training sample. Therefore, the output values of pixel values not seen in training are expected to vary relative to the expected outputs and were categorized if they did not conform exactly to the expected presence/absence values of 1 or 0. The prediction maps were then verified with the training data and validated using independent data. The optimal algorithm

characteristics were chosen based on the validation accuracy and conformance to expected output levels for the entire image. This algorithm was then used to simulate the remaining 17 subsets to produce a full map of the reserve.

3.4. *Comparison with traditional techniques*

It was hypothesized that the underlying restrictions and assumptions of traditional classification methodologies would not allow accurate classification of understorey features. To allow comparison to traditional techniques, supervised classifications of bamboo distribution were conducted on the 15 km × 15 km validation subset using ERDAS Imagine v. 8.3.1 (ERDAS 1999). The same training data used to train the neural network within the validation subset were used to gather supervised signatures. These signatures were categorized to allow maximum likelihood classifications and retained as single signatures for a minimum distance classification. This allowed testing of the effects of classification algorithms and merging of spectral signatures. Each method is a standard supervised classification approach. However, it was anticipated that the extreme topography and overstorey variation would require more than one signature to obtain accurate results. Utilizing different combinations of signatures allowed testing of these effects. The resulting output classes from each method were recombined into presence and absence categories. These binary classifications were then compared to the independent validation data to determine classification accuracy.

4. Results

4.1. *Design and performance evaluation*

Evaluation and comparison of the simulations were initially conducted on a 15 km × 15 km evaluation subset. For each algorithm where convergence was achieved, conformance to expected values, verification, and validation results were examined. It was found that the full TM data set (all six bands) was required for adequate convergence. Inputs using fewer bands converged more slowly or not at all. Adequate convergence was also not possible using an algorithm structure containing only one hidden layer. For comparison between algorithm structures using more than one hidden layer, verification and validation results were examined.

Prior to verification and validation analyses, the outputs were categorized into presence and absence values. This was necessary since the training data were not a fully representative sample of all land covers, combinations of land covers, topographic effects, and understorey conditions. Therefore, variations in the output value from the expected 1 or 0 were seen. For example, comparison of output values corresponding to training data plots showed value ranges of 0.99–1.00 as classification values for the presence of bamboo and only 0.00 for absence. However, output values for pixels where ground samples were available but not used for training showed a larger spread. In fact, for land covers (clouds, exposed rock, snow) where training data were not available, output values were as high as 2.5. In addition, since complete control even within sampled vegetation types and abiotic factors was not absolute, output values in vegetated areas ranged from 0–1.90. Therefore, when the entire image was simulated, output values from the network less than 0.50 or greater than 1.50 were considered absence and values greater than 0.50 and less than 1.50 were considered presence.

Algorithm verification was significantly higher when using at least 24 hidden nodes in the first layer and as high as 100% agreement for all convergence levels

Table 2. Influences of learning algorithms (BFGS quasi-newton (BFG) and Levenberg–Marquardt (LM)) and early stopping (mean square error levels of 1×10^{-5}, 1×10^{-8}, and 1×10^{-20}) on validation and verification accuracy (percentage).

Learning algorithm	MSE goal	Accuracy (verification)	Accuracy (validation)
LM	1×10^{-5}	100.0	80.0
LM	1×10^{-8}	100.0	62.2
LM	1×10^{-20}	100.0	55.6
BFG	1×10^{-5}	100.0	82.2
BFG	1×10^{-8}	100.0	75.6
BFG	1×10^{-20}	100.0	68.9

tested when using at least 24 nodes in the first layer and 48 nodes in the second hidden layer. The validation data for six algorithm architectures given in table 2 show the basic trend in network training. Validation results ranged from less than 50% from networks failing to fully converge (not shown) to 82% for the most optimal method shown. As shown in table 2, learning algorithms (e.g. Broyden-Fletcher-Goldfarb-Shanno (BFGS) quasi-newton (BFG) and Levenberg-Marquardt (LM)) had less influence on the overall accuracy compared to early stopping levels.

Examples of the outputs from the neural network algorithm tests on the 15 km × 15 km study area are shown in figure 4. Consistent areas of agreement among the outputs can be seen (figure 4 letterboxes) and represent trends in land cover such as major clearings and agriculture areas. The differences are less obvious. In tests run to convergence levels of 1×10^{-8} and 1×10^{-20} (figures 4(*b*) and (*c*)), land covers not represented in the training data are not classified within the expected 0–1 range of values and are noted as very bright features. Compared to the 1×10^{-5} trials (figure 4(*a*)), the latter image shows more consistent bamboo classification and better conformance to expected trends in output values (0–1). In addition, compared to overstorey classifications and knowledge of the region, the 1×10^{-5} method seems to retain land-use features (i.e. human appropriated areas, permanent rock, etc.) better. Based on these visual assessments and the validation results shown in table 1, the algorithm with two hidden layers, 24 and 48 hidden nodes, and convergence level of 1×10^{-5} with classification accuracy for the 15 km × 15 km study area of 80–82% was selected for full reserve analysis.

4.2. *Supervised classification*

Performing supervised classifications of the validation subset yielded consistently lower classification accuracy than the optimized neural network methods. Merging the individual signatures into two, presence and absence, signatures and then performing a maximum likelihood (ML) classification yielded a 71% classification accuracy based on the validation dataset. Using each of the individual signatures to perform a minimum distance classification resulted in a 69% classification accuracy of the bamboo. Subdividing the ML signatures into spectrally similar categories (i.e. similar aspect, slope, overstorey vegetation) produced similar results of 71% accuracy.

4.3. *Full reserve results*

Full reserve images of outputs from the neural net stopped at 1×10^{-5} are presented in figure 5. Figure 5(*a*) shows the mosaic of the 18 outputs. A comparison

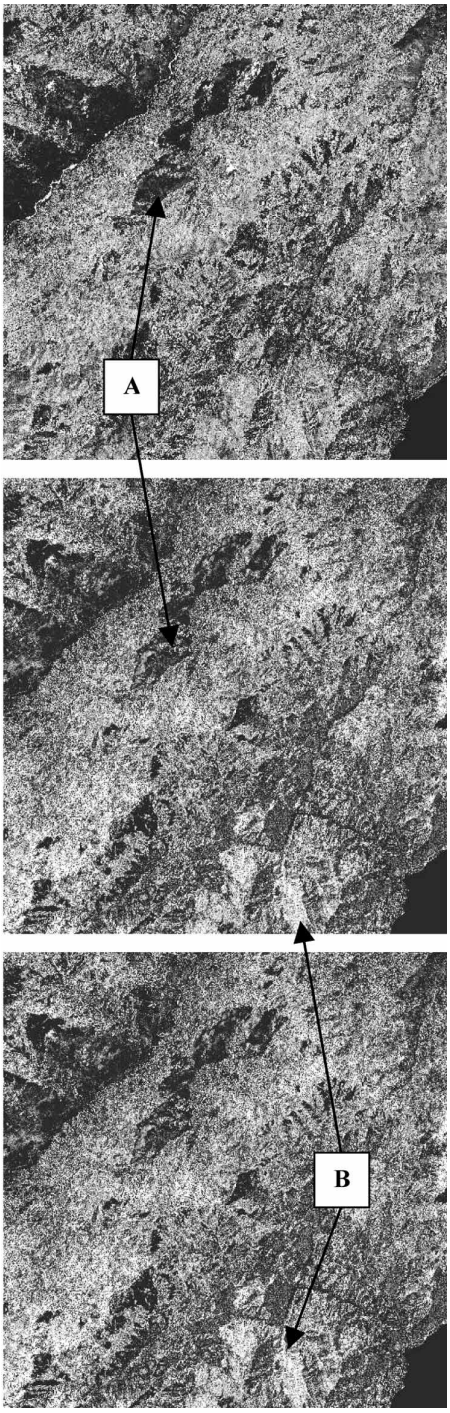

(*a*)

(*b*)

(*c*)

between the bamboo prediction map from the neural network to the field survey map is shown in figure 5(*b*) and shows an excellent correspondence between the predicted and surveyed distributions. Temporal differences of actual distribution between the surveyed and predicted bamboo maps are expected from natural

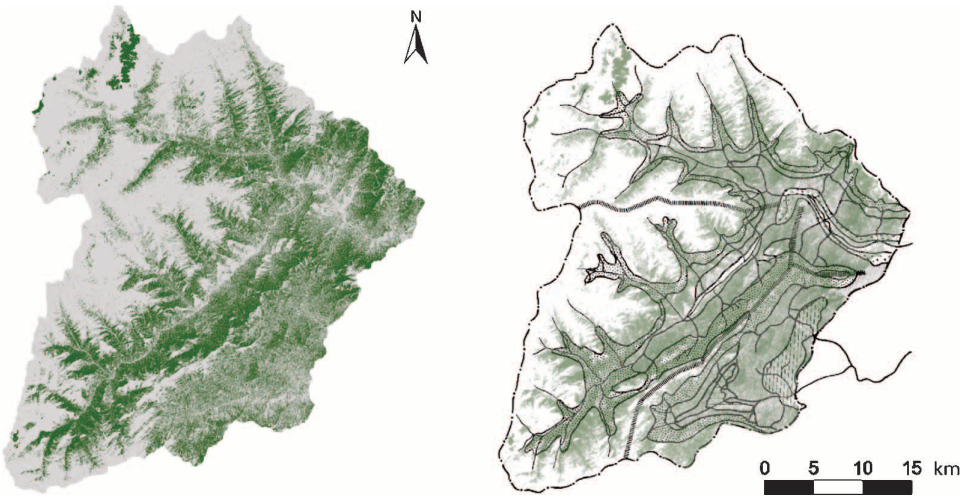

(*a*) (*b*)

Figure 5. Full reserve output maps from optimal algorithm input and structure. Input data were Landsat TM data excluding the thermal band and algorithm characteristics included two hidden layers with 24 and 48 nodes. The BFG learning algorithm with a convergence threshold of $\mathrm{MSE} = 1 \times 10^{-5}$ was used. (*a*) shows only the bamboo distribution, with green areas representing bamboo and grey areas the absence of bamboo. (*b*) shows the good correspondence of the neural network output as it compares to the full reserve output. Neural network bamboo prediction is shown as green overlaying ground survey distribution (for legend see figure 1(*b*)). Reprinted with permission from the University of Chicago Press.

dynamics and human disturbance, but since potential habitat is controlled by abiotic factors such as altitude, precipitation, and slope, overall distribution should be consistent through time. A confusion matrix of the full reserve output validation is presented in table 3. Overall accuracy based on all validation data was 80%. The matrix shows more clearly the correspondence between predicted and ground truth data and those pixels not being correctly categorized. Of particular note is the technique's inaccurate prediction of pixels containing bamboo as having an absence of bamboo, or false negatives. This category represents 75% of the incorrectly assigned pixels.

Further analyses examining factors influencing the errors and these false negatives in particular showed very interesting trends. For example, no relation between the percentage of canopy closure and prediction ability was found. In other words, the distribution of canopy closure for the miscategorized pixels was the same as all the data. It should be noted, however, that complete canopy closure was rare and bamboo was not found under 100% canopy closure. Nor was any relation of

Figure 4. Effects of algorithm structure are shown with variations in learning algorithm and error goal. (*a*) Output map from BFG training algorithm with convergence threshold of $\mathrm{MSE} = 1 \times 10^{-5}$. (*b*) and (*c*) Output maps from training algorithms with convergence thresholds of $\mathrm{MSE} = 1 \times 10^{-8}$ and 1×10^{-20}, respectively. Effects of generalization are apparent between methods using a 1×10^{-5} threshold (*a*) and LM 1×10^{-8} and 1×10^{-20} outputs (*b*) and (*c*). Better delineation of an agriculture area (inset A) using a 1×10^{-5} threshold and decreased generalization at 1×10^{-8} and 1×10^{-20} shown as brighter areas in (*b*) and (*c*) (inset B) do not conform to expected output values.

Table 3. Confusion matrix showing ground data values compared to predicted presence/absence from full-reserve analysis based on BFG 1×10^{-5} algorithm output using Landsat TM data. Numbers in parentheses represent those absence and presence validation points containing co-occurring grass (*) and shrubs (†), respectively.

Artificial neural network prediction	Ground data		
	Absence of bamboo	Presence of bamboo	Accuracy
Absence of bamboo	31	9(8†)	78%
Presence of bamboo	3(3*)	17	85%
Accuracy	91%	65%	Overall 80%

miscategorized pixels to the percentage bamboo found. Again, the distribution of miscategorized pixels was similar to that of all the data. However, significant trends were found in regards to co-occurring mid-storey and understorey vegetation within miscategorized pixels. In the case of 90% of the false negatives, a mid-storey, typically 2–5 m deciduous sub-canopy trees and shrubs, either partially covered and/or intermingled with the bamboo. In every case of the false positives, a grass understorey, with similar characteristics as *Bashania*, covered the forest floor. Ground data plots with co-occurring shrub in the case of false negatives and grass in the case of false positives in all represent 92% of the miscategorized pixels.

5. Conclusions and discussion

Data and algorithm requirements were found through testing various combinations of input, training data format, and algorithm architecture for successful neural network prediction of understorey bamboo presence/absence. The best results were obtained when using all six bands of the TM data as inputs. Infrared wavelengths have a greater canopy penetration compared to shorter wavelengths (Lillesand and Kiefer 1994). The TM sensor records information in three bands in the infrared, one in the near and two in the shortwave infrared. In addition, general application of the trained network was most accurate when stopped from reaching full convergence. Using this information, we were able to derive spatial distributions with significant correspondence to independent data. The results showed as high as 82% correspondence between predicted bamboo distribution and ground truth validation data.

In comparison to the maximum likelihood and minimum distance supervised classifications, clear gains were made using the neural network for bamboo classification. Relative to the observed distribution of bamboo, the supervised classifications seem to be more closely related to the general trends in the dominant vegetation. It is possible that the gains in the bamboo classification using the neural network are due to the ability of the neural net to more precisely learn trends in the dominant vegetation to that of the co-existence of bamboo. However, based on field observations (table 1) and classification errors we do not believe this is the case. While not providing conclusive evidence, trends in the classification and the lack of any discernable correlation of overstorey vegetation in forested regions to the existence of bamboo lead us to believe that the neural network is more capable of utilizing canopy gap and sub-canopy influences to more accurately classify understorey bamboo. The neural network is probably more capable of classifying minority features, adapting to the variable influences of changing canopy conditions, and accounting for the nonlinear effects of sub-canopy vegetation.

The misclassification trends discussed in the results and shown in table 3 lead us to believe that the neural network method is basing the classification, at least in part, on understorey vegetation to increase classification accuracy of understorey bamboo. We believe, for example, in the case of the false positives the neural network is falsely classifying other understorey grasses as bamboo. The grasses may be spectrally similar enough to the bamboo as to cause false positive classifications. In the case of the false negatives, it is possible that the co-occurring shrubs are simply masking understorey features. These pixels of co-occurring shrub and bamboo represent about 89% of the false negatives. The neural net may also be training against shrub containing plots as typically shrub dominated areas are devoid of bamboo. To test this, further data are being collected with emphasis on samples where there is co-occurring vegetation.

Data from other types of sensors may also contribute to these analyses and make parameterization of understorey conditions more applicable. Significant structural information (e.g. biomass and vertical distribution) can be inferred (and consequently some differentiation between structurally distinct vegetation types) from Synthetic Aperture Radar (SAR) (Luckman *et al*. 1997, Treuhaft and Siqueira 2000) and light detection and ranging (lidar) (Lefsky *et al*. 1999). We anticipate that the fusion of the increased biomass and structural information with the signature information available from optical sensor data may allow enhanced classifications and biophysical parameterization.

Canopy cover rarely exceeded 90% in Wolong and was on average around 56% during the middle of the growing season (Linderman *et al*. unpublished data). Neural network classification of canopy gap vegetation is, therefore, very feasible. The increased classification accuracy and correlation between miscategorized pixels and understorey vegetation suggest this is probably occurring here. The degree to which the neural net is capable of incorporating nonlinear effects such as multi-scattering and IR transmission due to sub-canopy vegetation is unknown. Further studies are necessary to test this and utilize this information if it is available. For example, to accurately classify the percentage cover and density of understorey vegetation, important data for many habitat models and mapping studies, methods sensitive to the nonlinear influences are most likely required. Determining the fraction of cover will require that the contribution of the sub-canopy vegetation be distinguishable and proportional to the fraction of sub-canopy vegetation. To this end, we are examining the relationship of the percentage cover of bamboo to optical remote sensing data using neural networks. However, further studies are needed as well. Analyses on the influence of training data set composition and size, neural network structure and characteristics, input data composition, among others are necessary to determine the influence of each of these aspects on understorey classification.

It is widely recognized that the understorey contains significant biomass and diversity of vegetation. However, it typically remains unclassified using traditional remote sensing techniques. The use of artificial neural networks to extract the complex information available from optical remote sensing data seems promising as a method to accurately classify understorey features. In addition, the neural network's ability to learn the complex trends in the data and to generalize across land covers make this method broadly applicable. Practical approaches to classifying understorey vegetation are needed for studies requiring more accurate information of biomass, biodiversity, and habitat conditions, as in the case for the endangered giant panda. We believe the results from this study at least point to a

need for further analyses on the influence of understorey vegetation on remote sensing data, information available from other data sets, and practical methods to use these data to classify understorey vegetation. Research in this area has the potential to provide a practical approach to classifying understorey vegetation and developing information on the quantity and spatial distribution of understorey vegetation species on a scale previously prohibitive.

Acknowledgments

We thank the Wolong Nature Reserve Administration, especially Zhang Hemin, for their kind assistance and support of our fieldwork. In addition, we thank Daniel Rutledge and James Brown (Department of Fisheries & Wildlife, Michigan State University) for their technical support. We gratefully acknowledge financial support from the National Aeronautics and Space Administration (NASA Earth Science Fellowship Award), the National Science Foundation (CAREER Award and Biocomplexity Grant), National Institute of Child Health and Human Development (R01 HD39789), American Association for Advancement of Sciences/The John D. and Katherine F. MacArthur Foundation, Michigan State University (All-University Research Initiation Grant, Global Competence Fund, Institute for International Agriculture), the National Natural Science Foundation of China, the Chinese Academy of Sciences, and China Bridges International (North America). We would also like to thank Dr Arthur Roberts and two anonymous reviewers for their constructive comments and suggestions.

References

ADAMS, J. B., SABOL, D. E., KAPOS, V., FILHO, R. A., ROBERTS, D. A., SMITH, M. O., and GILLESPIE, A. R., 1995, Classification of multispectral images based on fractions of endmembers: application to land-cover change in the Brazilian Amazon. *Remote Sensing of Environment*, **52**, 137–154.

ASNER, G. P., and LOBELL, D. B., 2000, A biogeophysical approach for automated SWIR unmixing of soils and vegetation. *Remote Sensing of Environment*, **74**, 99–112.

ATKINSON, P. M., and TATNALL, A. R. L., 1997, Neural networks in remote sensing. *International Journal of Remote Sensing*, **18**, 699–709.

BAUSCH, W. C., 1993, Soil background effects on reflectance-based crop coeffecients for corn. *Remote Sensing of Environment*, **46**, 213–222.

BOREL, C. C., and GERSTL, S. A. W., 1994, Nonlinear spectral mixing models for vegetative and soil surfaces. *Remote Sensing of Environment*, **47**, 403–416.

CARPENTER, G. A., GOPAL, S., MACOMBER, S., MARTENS, S., and WOODCOCK, C. E., 1999, A neural network method for mixture estimation for vegetation mapping. *Remote Sensing of Environment*, **70**, 138–152.

CROSS, A. M., SETTLE, J. J., DRAKE, N. A., and PAIVINEN, R. T. M., 1991, Subpixel measurement of tropical forest cover using AVHRR data. *International Journal of Remote Sensing*, **12**, 1119–1129.

DE WULF, R. R., GOOSSENS, R. E., MACKINNON, J. R., and WU, S. C., 1988, Remote sensing for wildlife management: giant panda habitat mapping from LANDSAT MSS images. *Geocarto International*, **1**, 41–50.

ERDAS, 1999, Imagine, version 8.3.1. Atlanta, GA, USA.

FOODY, G. M., 1996, Relating the land-cover composition of mixed pixels to artificial neural network classification output. *Photogrammetric Engineering and Remote Sensing*, **62**, 491–499.

FOODY, G. M., and ARORA, M. K., 1997, An evaluation of some factors affecting the accuracy of classification by an artificial neural network. *International Journal of Remote Sensing*, **18**, 799–810.

GHITTER, G. S., HALL, R. J., and FRANKLIN, S. E., 1995, Variability of Landsat Thematic Mapper data in boreal deciduous and mixed-wood stands with conifer understorey. *International Journal of Remote Sensing*, **16**, 2989–3002.

GILABERT, M. A., GARCÍA-HARO, F. J., and MELIÁ, J., 2000, A mixture modeling approach to estimate vegetation parameters for heterogeneous canopies in remote sensing. *Remote Sensing of Environment*, **72**, 328–345.

GUYOT, G., and RIOM, D. G. J., 1989, Factors affecting the spectral response of forest canopies: A review. *Geocarto International*, **3**, 3–18.

HUETE, A. R., JACKSON, R. D., and POST, D. F., 1985, Spectral response of a plant canopy with different soil backgrounds. *Remote Sensing of Environment*, **17**, 37–53.

JOHNSON, K. G., SCHALLER, G. B., and HU, J., 1988, Responses of giant pandas to a bamboo die-off. *National Geographic Research*, **4**, 161–177.

KEELEY, J. E., and BOND, W. J., 1999, Mast flowering and semelparity in bamboos: The bamboo fire cycle hypothesis. *The American Naturalist*, **154**, 383–391.

LAW, B. E., and WARING, R. H., 1994, Remote Sensing of Leaf Area Index and radiation intercepted by understorey vegetation. *Ecological Applications*, **4**, 272–279.

LEFSKY, M. A., PARKER, G. G., SPIES, T. A., HARDING, D., COHEN, W. B., and ACKER, S. A., 1999, Lidar remote sensing of the canopy structure and biophysical properties of Douglas-fir western hemlock forests. *Remote Sensing of Environment*, **70**, 339–361.

LILLESAND, T. M., and KIEFER, R. W., 1994, *Remote Sensing and Image Interpretation*, 3rd edn (New York: John Wiley & Sons).

LIU, J., OUYANG, Z., YANG, Z., TAYLOR, W., GROOP, R., TAN, Y., and ZHANG, H., 1999a, A framework for evaluating the effects of human factors on wildlife habitat: The case of giant pandas. *Conservation Biology*, **13**, 1360–1370.

LIU, J., OUYANG, Z., TAN, Y., YANG, J., and ZHANG, H., 1999b, Changes in human population structure: Implications for biodiversity conservation. *Population and Environment*, **21**, 45–58.

LIU, J., LINDERMAN, M., OUYANG, Z., AN, L., YANG, J., and ZHANG, H., 2001, Ecological degradation in protected areas: the case of Wolong Nature Reserve for giant pandas. *Science*, **292**, 98–101.

LUCKMAN, A., YANASSE, C. C. F., FRERY, A. C., BAKER, J., and KUPLICH, T. M., 1997, A study of the relationship between radar backscatter and regenerating tropical forest biomass for spaceborne SAR instruments. *Remote Sensing of Environment*, **60**, 1–13.

MACARTHUR, R. H., and MACARTHUR, J. W., 1961, On bird species diversity. *Ecology*, **42**, 594–598.

MORAIN, S. A., 1986, Surveying China's agricultural resources: patterns and progress from space. *Geocarto International*, **1**, 15–24.

NEMANI, R., PIERCE, L., RUNNING, S., and BAND, L., 1993, Forest ecosystem processes at the watershed scale: sensitivity to remotely-sensed Leaf Area Index estimates. *International Journal of Remote Sensing*, **14**, 2519–2534.

ODUM, E. P., 1971, *Fundamentals of Ecology* (Philadelphia: W. B. Saunders Company).

PORWALL, M. C., and ROY, P. S., 1991, Attempted understorey characterization using aerial photography in Kanha National Park, Madhya Pradesh, India. *Environmental Conservation*, **18**, 45–50.

QI, J., WELTZ, M., HUETE, A. R., SOROOSHIAN, S., BRYANT, R., KERR, Y. H., and MORAN, M. S., 2000, Leaf area index estimates using remotely sensed data and BRDF models in a semiarid region. *Remote Sensing of Environment*, **73**, 18–30.

RANSON, K. J., DAUGHTRY, C. S. T., and BIEHL, L. L., 1986, Sun angle, view angle, and background effects on spectral response of simulated balsam fir canopies. *Photogrammectric Engineering and Remote Sensing*, **52**, 649–658.

REID, D. G., HU, J., DONG, S., WANG, W., and HUANG, Y., 1989, Giant panda *Ailuropoda melanoleuca* behaviour and carrying capacity following a bamboo die-off. *Biological Conservation*, **49**, 85–104.

ROBERTS, D. A., SMITH, M. O., and ADAMS, J. B., 1993, Green vegetation, nonphotosynthetic vegetation, and soils in AVIRIS data. *Remote Sensing of Environment*, **44**, 255–269.

ROUGHGARDEN, J., RUNNING, S. W., and MATSON, P. A., 1991, What does remote sensing do for ecology? *Ecology*, **72**, 1918–1922.

SCHALLER, G. B., HU, J., PAN, W., and ZHU, J., 1985, *The Giant Pandas of Wolong*, (Chicago: University of Chicago Press).

SPANNER, M. A., PIERCE, L. L., PETERSON, D. L., and RUNNING, S. W., 1994, Remote sensing of temperate coniferous forest leaf area index: the influence of canopy

closure, understorey vegetation and background reflectance. *Ecological Applications*, **4**, 258–271.

STENBACK, J. M., and CONGALTON, R. G., 1990, Using Thematic Mapper imagery to examine forest understorey. *Photogrammetric Engineering and Remote Sensing*, **56**, 1285–1290.

TAYLOR, A. H., and QIN, Z., 1997, The dynamics of temperate bamboo forests and panda conservation in China. In *The Bamboos*, edited by G. P. Chapman (San Diego: Harcourt Brace & Company), pp. 189–211.

The MATHWORKS INC., 1999, Matlab, version 5.3.1. Natick, MA, USA.

TREUHAFT, R. N., and SIQUEIRA, P. R., 2000, Vertical structure of vegetated land surfaces from interferometric and polarimetric radar. *Radio Science*, **35**, 141–177.